EUROPEAN COOPERATION

IN THE FIELD OF SCIENTIFIC

AND TECHNICAL RESEARCH

EURO-COST

COST 273 TD(03)199

Prague, Czech Republic

2003/Sept/24-26

SOURCE: Institute of Communications and Measurement Engineering
Dept. of Electrical Engineering and Information Technology
Ilmenau University of Technology
Germany

Performance Evaluation of Real Antenna Arrays for High-Resolution DoA Estimation in Channel Sounding

Part 1: Channel Parameter Resolution Limits

Part 2: Experimental ULA Measurement Results

Markus Landmann

Technische Universität Ilmenau

FG EMT

POB 100565

98684 Ilmenau

Germany

Phone: + 49-3677691160

Fax: + 49-3677691113

Email: markus.landmann@tu-ilmenau.de

Performance Evaluation of Real Antenna Arrays for High-Resolution DoA Estimation in Channel Sounding

Part 1: Channel Parameter Resolution Limits

M. Landmann, A. Richter, R.S.Thoma

Ilmenau University of Technology, Ilmenau, Germany
markus.landmann@tu-ilmenau.de

Abstract: *Several high-resolution parameter estimation algorithms (such as ESPRIT, ML, SAGE, RIMAX) have been applied to directional channel parameter estimation in channel sounding. However, variance and reliability of the estimation results are not often clearly defined in practical environments. Especially, imperfections, mutual coupling, and residual calibration errors of real antenna arrays impose limits to the DoA parameter estimation performance. This is especially true if resolution of coherent wave fronts is involved which is in general the case for real-time channel sounding. In the first part of this paper we derive the Cramer-Rao-Lower-Bound (CRLB) of an unbiased direction-of-arrival (DoA) estimator. The CRLB indicates the minimum achievable parameter variance which can not be outperformed by any parameter estimator. It is shown that the required derivatives of the observations with respect to the DoA and path weight parameters can be deduced from a properly defined calibration data model.*

1 Introduction

The interest in the multidimensional structure of the mobile radio channel is growing rapidly. For optimum design and performance evaluation of transmission systems using antenna arrays and sophisticated space-time algorithms we need realistic directional channel models. The recent MIMO system verve calls for double-directional channel models [1]. It is commonly understood that high-resolution multidimensional channel sounding measurements [2] are required to study the multidimensional wave propagation mechanism and to deduce and verify channel models. This is especially true, if the multidimensional channel parameters are directly estimated from MIMO sounding records in representative propagation environments as recently proposed in [3]. These multiple dimensions are DoA and DoD (in terms of azimuth and elevation at both the transmitter and the receiver), the time delay of arrival and the Doppler shift of any relevant propagation path. Furthermore, any path is described by a 4x4 polarimetric complex path weight matrix. This parametric path model roughly describes the underlying data model which is used for high-resolution parameter estimation from measurements. See also [4] for a recent extension of this data model.

Several high-resolution channel parameter estimation algorithms have been reported for this application, mainly based on ESPRIT [5], SAGE [6] [7] [8] and RIMAX [9] which essentially is a gradient based Maximum Likelihood parameter estimator. See also [10] for first real-time, high-resolution joint double directional measurement based on the multidimensional unitary ESPRIT (note the real-time here means that the time variance of the channel is fully taken into account). However, resolution and reliability of these estimation procedures are not often clearly defined. From huge experience with measured data, e.g., it has been observed, that a high-resolution channel parameter estimator may yield results that approximates the observed data very well. Although, closer inspection of the data often shows that there is no physical relevance. One typical example is that a small physical path may be approximated by two almost equal magnitude opposite but physically meaningless weights (line splitting). Apparently, this is often a result of model order over-estimation. It was also observed that the variance of this estimates is typically very high.

Obviously, the most severe problems arise if coherent wave-fronts are involved which is in general the case for real-time channel sounding were we aim to estimate one set of multidimensional parameters from only one single snap-shot. See [5] and [11] for a first demonstration of empirical resolution limits in coherent wave fields.

Since resolution and reliability of high-resolution parameter estimation (besides of SNR) has always something to do with calibration or precise knowledge of the measurement device parameters, it seems quite clear that the quality of the antenna arrays may be considered as the weakest point in the performance of high-resolution channel sounding. The performance of a real antenna array is always susceptible to various imperfections, mutual element coupling and residual calibration errors. Moreover, the observed spatial aperture, which has strong influence to resolution, is severely limited by the available array size and data model constraints.

In this paper we will derive the fundamental limitations on the achievable DoA and path weight variance in terms of the Cramer-Rao-Lower-Bound (CRLB) [12] [13] of an unbiased DoA parameter estimator. The CRLB indicates the minimum achievable parameter variance which can not be outperformed by any possible parameter estimator. The advantage of our method is that it completely relies on measured antenna characteristics. The data base required is the same which is used as reference data for RIMAX or SAGE based channel parameter estimators. Therefore we also introduce this calibration data model that has the advantage to deliver the required derivatives of the observations with respect to the DoA and path weight parameters which we need for RIMAX gradient calculation and Fisher information matrix construction. In the part I of this paper we also show analytic results for simple Circular Uniform Beam Array and in part II [16] we will provide measured data.

2 Cramer-Rao-Lower-Bound (CRLB)

The Cramer-Rao-Lower-Bound is the minimum variance of an unbiased channel parameter estimator. The variances of the channel parameters such as angle of arrival (resp. departure) $\Omega(\vartheta, \varphi)$ and of the complex path weights γ are defined as the diagonal elements of the inverse Fisher-Information-Matrix (FIM). The FIM is given by the covariance matrix of the L first order derivatives of the observed data vector ((2.3) and (2.2)) with respect to the parameters $\boldsymbol{\theta}$ of the K paths in the given scenario:

$$\boldsymbol{\theta}^{[1\times L]} = \left[\begin{bmatrix} \vartheta_1 & \cdots & \vartheta_K \end{bmatrix} \begin{bmatrix} \varphi_1 & \cdots & \varphi_K \end{bmatrix} \begin{bmatrix} \mathrm{Re}\{\gamma_1\} & \cdots & \mathrm{Re}\{\gamma_K\} \end{bmatrix} \begin{bmatrix} \mathrm{Im}\{\gamma_1\} & \cdots & \mathrm{Im}\{\gamma_K\} \end{bmatrix} \right] \quad (2.1)$$

The angles elevation ϑ and azimuth φ are defined in the spherical coordinate system. The observed data of the channel scenario is

$$\mathbf{x}^{[M\times 1]}(\boldsymbol{\theta}, \mathbf{n}) = \mathbf{s}^{[M\times 1]}(\boldsymbol{\theta}) + \mathbf{n}^{[M\times 1]} \quad (2.2)$$

whereby $\mathbf{n}$ denotes the noise vector and

$$\mathbf{s}(\boldsymbol{\theta}) = \sum_{k=1}^{K} \gamma_k \cdot \mathbf{b}(\Omega_k) \tag{2.3}$$

results from the superposition of all K paths weighted by the according complex polarimetric array response $\mathbf{b}(\Omega_k)$. For a known $\boldsymbol{\theta}$ the probability density function of the described problem is:

$$pdf\left(\mathbf{x} \mid (\boldsymbol{\theta}, \mathbf{R}_{nn})\right) = \frac{1}{\pi^M \det(\mathbf{R}_{nn})} \mathrm{e}^{-(\mathbf{x}-\mathbf{s}(\boldsymbol{\theta}))^H \cdot \mathbf{R}_{nn}^{-1} \cdot (\mathbf{x}-\mathbf{s}(\boldsymbol{\theta}))}. \tag{2.4}$$

In the case of independent identical normal distributed noise in the real and imaginary part with a standard deviation σ, the noise covariance matrix is defined as

$$\mathbf{R}_{nn} = \mathrm{E}\{\mathbf{n}^H \cdot \mathbf{n}\} = \sigma^2 \cdot \mathbf{I}. \tag{2.5}$$

To calculate the CRLB of a real antenna array with respect to the parameters azimuth φ and elevation ϑ we need the complex polarimetric array response $\mathbf{b}(\Omega_k)$ and its derivatives. Simple storing of the sampled $\mathbf{b}(\Omega_k)$ is computationally unattractive. Instead we define an antenna data model which maps the measured $M_{\mathrm{Rx,Tx}}$ beam patterns $\mathbf{b}(\varphi, \vartheta)$ to what we call the effective aperture distribution function (EADF) $\mathbf{g}(f_1, f_2)$ by Fourier transform. From antenna theory it is well known that with specific geometric transformations the far field characteristic corresponds by Fourier transform to the aperture field distribution. However, here we do not aim to electromagnetic antenna design. Therefore we can ignore any projection of the field to a physical antenna aperture. Instead we simply use this transformed beam patterns as an antenna array calibration data model. As we will clearly see later from the measured example, one advantage of this approach is that the EADF typically is concentrated to a very small support. This seems to result from the related physical meaning of the aperture distribution which should be somewhat limited in space. Another advantage is that the derivatives can be exactly calculated. Actually, because of the periodic nature of the beam patterns in azimuth and elevation, the EADF can be considered as two-dimensional Fourier series expansion of the beam pattern.

In the sequel we discuss some further steps to be considered throughout EADF estimation. This model describes the array manifold for a certain frequency f or for some narrow bandwidth around a center frequency f_0. The maximum bandwidth is limited by the desired precision of the model's approximation of the measured data. For wideband applications it may be necessary to divide the whole frequency range in several segments. The following description characterizes only one of these segments or considers the single frequency case.

The complex polarimetric beam patterns $\mathbf{b}(\Omega_k)$, in general from both vertical and horizontal stimulation [8] [9] are measured in a well defined propagation environment which should be an anechoic chamber whereby the pivot point of the antenna array is located in the origin of the spherical coordinate system. The zero azimuth and elevation direction is defined by the calibration setup and marked by laser pointer. The measured beam patterns are discrete in azimuth $\varphi = (-\pi \ldots \Delta\varphi \ldots \pi - \Delta\varphi)$ and elevation $\vartheta = (0 \ldots \Delta\vartheta \ldots \pi)$. Due to the periodicity of the beam patterns in 2π it is possible to use the discrete Fourier transform to transfer $\mathbf{b}(\varphi, \vartheta)$ to the effective aperture domain $\mathbf{g}(f_1, f_2)$ without any leakage error. The beam pattern $\mathbf{b}(\varphi, \vartheta, m)$ of the antenna m is stored in the matrix $\mathbf{B}^{[N_1' \times N_2]}$ (the superscript [.] denotes the dimension of the matrix). The periodicity of the beam pattern has to be ensured in both dimensions. If the azimuth response is measured in 2π, elevation characterization in π is enough to completely describe the spherical beam pattern. However, for two-dimensional signal processing this is not enough and we have to construct a fully 2D-periodic data structure by some periodic extension. The 2D-periodic beam pattern $\mathbf{B}_\mathbf{p}^{[N_1 \times N_2]}$ is defined as

$$\mathbf{B}_\mathbf{p}^{[N_1 \times N_2]} = \begin{bmatrix} \mathbf{B} \\ \mathbf{B}_\mathrm{r} \end{bmatrix};\; N_1' = \left(\frac{\pi}{\Delta\vartheta} + 1 \right);\; N_2 = \frac{2\pi}{\Delta\varphi};\; N_1 = 2(N_1' - 1) \qquad (2.6).$$

Half of the data of $\mathbf{B}_\mathbf{p}^{[N_1 \times N_2]}$ is redundant, since the matrix

$$\mathbf{B}_\mathrm{r}^{[N_1' - 2 \times N_2]} = \begin{bmatrix} -\mathbf{B}_1 & -\mathbf{B}_2 \end{bmatrix} \qquad (2.7)$$

is just the same data as $-\mathbf{B}$ shifted about 180° in azimuth and flipped in elevation direction. This is caused by the redundancy of spherical coordinate system when elevation crosses the poles (0° and 180° elevation). In essence, it is a shift of 180° in azimuth and a rotation of the polarization vector about 180 degrees. The resulting matrix structure can be seen in Fig. 1. The following equations effect the exact shifting and flipping operation to calculate the matrix $\mathbf{B}_\mathrm{r}$ of the 2D-periodic beam pattern $\mathbf{B}_\mathbf{p}$.

$$\mathbf{B}_1^{[N_1' - 2 \times N_2/2]} = \begin{bmatrix} \mathbf{0} & \mathbf{\Pi}^{[N_1' - 2 \times N_1 - 2]} & \mathbf{0} \end{bmatrix} \cdot \mathbf{B}^{[N_1' \times N_2]} \cdot \begin{bmatrix} \mathbf{0}^{[N_2/2 \times N_2/2]} \\ \mathbf{I}^{[N_2/2 \times N_2/2]} \end{bmatrix} \qquad (2.8)$$

$$\mathbf{B}_2^{[N_1' - 2 \times N_2/2]} = \begin{bmatrix} \mathbf{0} & \mathbf{\Pi}^{[N_1' - 2 \times N_1' - 2]} & \mathbf{0} \end{bmatrix} \cdot \mathbf{B}^{[N_1' \times N_2]} \cdot \begin{bmatrix} \mathbf{I}^{[N_2/2 \times N_2/2]} \\ \mathbf{0}^{[N_2/2 \times N_2/2]} \end{bmatrix} \qquad (2.9).$$

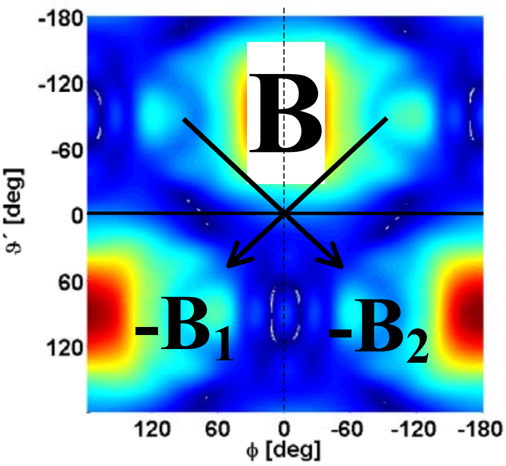

Fig.1 Beam pattern $\mathbf{B}_\mathbf{p}^{[N_1 \times N_2]}$ (periodic in azimuth and elevation)

By discrete Fourier transform using the elevation transformation matrix

$$\mathbf{D}_1 = \mathrm{e}^{-\mathrm{j}2\pi\cdot\vartheta'\cdot\mathbf{f}_1} = \mathrm{e}^{-\mathrm{j}2\pi\boldsymbol{\mu}_1\Delta f_1\cdot\mathbf{n}_1\Delta\vartheta'} = \mathrm{e}^{-\mathrm{j}2\pi\cdot\boldsymbol{\mu}_1\mathbf{n}_1/N_1}; \quad \Delta\vartheta' = \frac{2\pi}{N_1}; \quad \Delta f_1 = \frac{1}{2\pi} \tag{2.10}$$

$$\mathbf{n}_1 = \boldsymbol{\mu}_1^{\mathrm{T}} = \left[\frac{-N_1}{2} \quad \ldots \quad \frac{N_1}{2}-1\right]; \; \vartheta' = \vartheta - \pi \tag{2.11}$$

and the azimuth transformation matrix

$$\mathbf{D}_2 = \mathrm{e}^{-\mathrm{j}2\pi\cdot\varphi\cdot\mathbf{f}_2} = \mathrm{e}^{-\mathrm{j}2\pi\boldsymbol{\mu}_2\Delta f_2\cdot\mathbf{n}_2\Delta\varphi} = \mathrm{e}^{-\mathrm{j}2\pi\cdot\boldsymbol{\mu}_2\mathbf{n}_2/N_2}; \quad \Delta\varphi = \frac{2\pi}{N_2}; \quad \Delta f_2 = \frac{1}{2\pi} \tag{2.12}$$

$$\mathbf{n}_2^{\mathrm{T}} = \boldsymbol{\mu}_2 = \left[-\frac{N_2}{2} \quad \ldots \quad \frac{N_2}{2}-1\right] \tag{2.13}$$

we get the EADF of the *m*–th antenna

$$\mathbf{G}_m = \frac{1}{\sqrt{N_1 \cdot N_2}}\mathbf{D}_1 \cdot \mathbf{B}_\mathbf{p} \cdot \mathbf{D}_2 \tag{2.14}$$

In case of an over-sampling of the beam pattern in the angular domain this transformation maybe used to achieve a data compression (Fig. **2** (a)). The required size $N_{a1} \times N_{a2}$ of the effective aperture is determined by the measured samples in the angular domain, the beam width of the antenna and the signal to noise ratio (SNR) of the calibration measurement (Fig. 2 (b)). The 2D beam width somewhat limits the required EADF size to a finite support area. For the marginal case of the isotropic radiator the effective aperture is just a Dirac impulse.

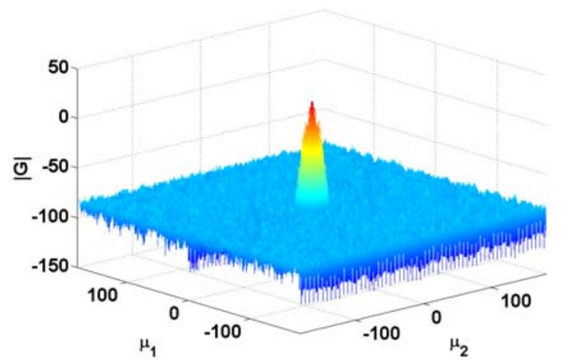

(a) Fourier transform of the over-sampled beam pattern

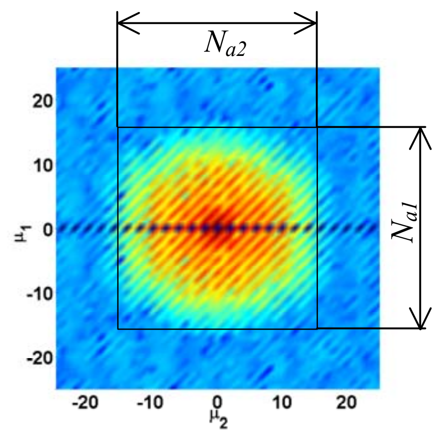

(b) finite EADF support

Fig. 2 EADF as calculated from the periodic beam pattern martix

Only the data of the finite support area are kept for further processing. This results in a considerable data reduction and even measurement noise reduction. The EADF shape (if not well concentrated) can also investigated to identify wrong calibration measurement data. The complex exponentials for the reduced EADF transformed to the beam domain are defined for elevation and azimuth by

$$\mathbf{d}_{b1}(\vartheta') = \mathrm{e}^{\mathrm{j}\vartheta' \cdot \boldsymbol{\mu}_1^{\mathrm{T}}} \tag{2.15}$$

$$\mathbf{d}_{b2}(\varphi) = \mathrm{e}^{\mathrm{j}\boldsymbol{\mu}_2 \cdot \varphi} \tag{2.16}$$

with the vectors $\boldsymbol{\mu}_1, \boldsymbol{\mu}_2$ and the required number of samples $N_{\mathrm{a}1}, N_{\mathrm{a}2}$ (Fig. 2 (b))

$$\boldsymbol{\mu}_1^{\mathrm{T}} = \begin{bmatrix} \frac{-(N_{\mathrm{a}1}-1)}{2} & \cdots & \frac{(N_{\mathrm{a}1}-1)}{2} \end{bmatrix} \tag{2.17}$$

$$\boldsymbol{\mu}_2^{\mathrm{T}} = \begin{bmatrix} \frac{-(N_{\mathrm{a}2}-1)}{2} & \cdots & \frac{(N_{\mathrm{a}2}-1)}{2} \end{bmatrix} \tag{2.18}$$

The beam pattern and its derivatives for an arbitrary azimuth/elevation angle pair $\Omega(\vartheta, \varphi)$ are defined by the following equations:

$$\mathbf{b}(\vartheta, \varphi, m) = \frac{1}{\sqrt{N_{\mathrm{a}1} \cdot N_{\mathrm{a}2}}} \mathbf{d}_{b1} \cdot \mathbf{G}_m \cdot \mathbf{d}_{b2} \tag{2.19}$$

$$\frac{\partial \mathbf{b}(\vartheta, \varphi, m)}{\partial \vartheta} = \frac{1}{\sqrt{N_{\mathrm{a}1} \cdot N_{\mathrm{a}2}}} \mathrm{j} \cdot \mathbf{d}_{b1} \cdot \mathrm{diag}\{\boldsymbol{\mu}_1^{\mathrm{T}}\} \cdot \mathbf{G}_m \cdot \mathbf{d}_{b2} \tag{2.20}$$

$$\frac{\partial \mathbf{b}(\vartheta, \varphi, m)}{\partial \varphi} = \frac{1}{\sqrt{N_{\mathrm{a}1} \cdot N_{\mathrm{a}2}}} \mathrm{j} \cdot \mathbf{d}_{b1} \cdot \mathbf{G}_m \cdot \mathrm{diag}\{\boldsymbol{\mu}_2^{\mathrm{T}}\} \cdot \mathbf{d}_{b2} \tag{2.21}$$

We get the equations for an antenna array with M antennas:

$$\mathbf{b}(\vartheta, \varphi)^{[M \times 1]} = \frac{1}{\sqrt{N_{\mathrm{a}1} \cdot N_{\mathrm{a}2}}} \cdot \begin{bmatrix} \mathrm{vec}\{\mathbf{G}_1\}^{\mathrm{T}} \\ \vdots \\ \mathrm{vec}\{\mathbf{G}_{M_{\mathrm{Rx}}}\}^{\mathrm{T}} \end{bmatrix} \cdot \mathrm{vec}\{\mathbf{d}_{b1}^{\mathrm{T}}(\vartheta) \cdot \mathbf{d}_{b2}^{\mathrm{T}}(\varphi)\} \tag{2.22}$$

$$\mathbf{b}(\vartheta, \varphi)^{[M \times 1]} = \frac{1}{\sqrt{N_{\mathrm{a}1} \cdot N_{\mathrm{a}2}}} \cdot \boldsymbol{\Gamma}^{[M_{\mathrm{Rx}} \times N_1 \cdot N_2]} \cdot \mathbf{d}_b^{[N_1 \cdot N_2 \times 1]}(\vartheta, \varphi) \tag{2.23}$$

The derivatives of the beam patterns $\mathbf{b}(\vartheta, \varphi)$ with respect to the azimuth and elevation angle are calculated equivalently using the derivatives of the complex exponentials $\frac{\partial \mathbf{d}_b(\vartheta, \varphi)}{\partial \vartheta}$ and $\frac{\partial \mathbf{d}_b(\vartheta, \varphi)}{\partial \varphi}$ instead of $\mathbf{d}_b$.

$$\frac{\partial \mathbf{b}(\vartheta,\varphi)^{[M\times 1]}}{\partial \varphi} = \frac{1}{\sqrt{N_{\mathrm{a}1}\cdot N_{\mathrm{a}2}}}\cdot \mathbf{\Gamma}^{[M_{\mathrm{Rx}}\times N_1\cdot N_2]}\cdot \frac{\partial \mathbf{d}_b^{[N_1\cdot N_2\times 1]}(\vartheta,\varphi)}{\partial \varphi} \tag{2.24}$$

$$\frac{\partial \mathbf{b}(\vartheta,\varphi)^{[M\times 1]}}{\partial \vartheta} = \frac{1}{\sqrt{N_{\mathrm{a}1}\cdot N_{\mathrm{a}2}}}\cdot \mathbf{\Gamma}^{[M_{\mathrm{Rx}}\times N_1\cdot N_2]}\cdot \frac{\partial \mathbf{d}_b^{[N_1\cdot N_2\times 1]}(\vartheta,\varphi)}{\partial \vartheta} \tag{2.25}$$

The derivatives with respect to the real and imaginary part of the parameters of the *k*-th path weight result from

$$\frac{\partial \mathbf{s}(\boldsymbol{\theta})}{\partial\,\mathrm{Re}\{\gamma_k\}} = \mathbf{b}(\Omega_k) \tag{2.26}$$

$$\frac{\partial \mathbf{s}(\boldsymbol{\theta})}{\partial\,\mathrm{Im}\{\gamma_k\}} = \mathrm{j}\cdot\mathbf{b}(\Omega_k) \qquad (2.27).$$

The matrix of the first order derivatives is given by:

$$\mathbf{A} = \begin{bmatrix} \frac{\partial \mathbf{s}(\boldsymbol{\theta})}{\partial \theta_1} & \cdots & \frac{\partial \mathbf{s}(\boldsymbol{\theta})}{\partial \theta_L} \end{bmatrix} \qquad (2.28).$$

The real part of the covariance matrix of $\mathbf{A}$ is proportional to the Fisher-Information-Matrix (FIM)

$$\mathbf{J} = 2\cdot\mathrm{Re}\left\{\mathbf{A}^{\mathrm{H}}\cdot\mathbf{R}_{nn}^{-1}\cdot\mathbf{A}\right\} \tag{2.29}$$

whereby the diagonal elements of the inverse FIM represent the CRLB of the *L* parameters

$$\mathrm{CRLB}(\boldsymbol{\theta}) = \mathrm{diag}\left\{\mathbf{J}^{-1}\right\} = \begin{bmatrix}\sigma_1^2 & \cdots & \sigma_L^2\end{bmatrix} \tag{2.30}$$

and the non diagonal elements of the inverse FIM denote the co-variances. In case of uncorrelated parameters these non-diagonal elements are zero. With a single path test scenario it is possible to calculate the maximum possible resolution dependent on a certain SNR. Normally the non-diagonal elements are zero in this case. In more difficult scenarios with two or more coherent paths the non diagonal elements will not disappear. This indicates a correlation between the parameters of the different paths and will increase the overall variances of the path parameters.

3 CRLBs of a simple scenario using a CUBA array

In this section the CRLBs for a simple single path scenario using a ideal Circular Uniform Beam Array [14] are analytically derived. The CUBA is used for simplicity. The one-dimensional EADF of the CUBA is defined as

$$\mathbf{\Gamma}_{\mathrm{CUBA}}^{[M_{\mathrm{Rx}}\times N_2]} = \frac{1}{\sqrt{N_2}}\,\mathrm{e}^{-\mathrm{j}\cdot\begin{bmatrix}0\\ \vdots\\ M_{\mathrm{Rx}}-1\end{bmatrix}\cdot\varphi_0\cdot\boldsymbol{\mu}_2^{\mathrm{T}}} \quad ;\ \varphi_0 = \frac{2\pi}{M_{\mathrm{Rx}}} \qquad (3.1).$$

To calculate the Fisher Information Matrix, the first order derivatives with respect to the parameters azimuth φ_1

$$\frac{\partial \mathbf{s}(\boldsymbol{\theta})}{\partial \varphi_1} = \gamma_1 \cdot \mathrm{j} \cdot \boldsymbol{\Gamma}_{\mathrm{CUBA}} \cdot \mathrm{diag}(\mu_2) \cdot \mathbf{d}_{\mathrm{b2}}(\varphi_1) \qquad (3.2),$$

and the real and imaginary part of the complex path weight γ_1

$$\frac{\partial \mathbf{s}(\boldsymbol{\theta})}{\partial \operatorname{Re}\{\gamma_1\}} = \boldsymbol{\Gamma}_{\mathrm{CUBA}} \cdot \mathbf{d}_{\mathrm{b2}}(\varphi_1) \qquad (3.3)$$

$$\frac{\partial \mathbf{s}(\boldsymbol{\theta})}{\partial \operatorname{Im}\{\gamma_1\}} = \mathrm{j} \cdot \boldsymbol{\Gamma}_{\mathrm{CUBA}} \cdot \mathbf{d}_{\mathrm{b2}}(\varphi_1) \qquad (3.4)$$

have to be determined. Assuming independent identical normal distributed noise in real and imaginary part with a standard deviation of σ and a simplified expression for the necessary covariance matrix of $\boldsymbol{\Gamma}_{\mathrm{CUBA}}$:

$$\boldsymbol{\Gamma}_{\mathrm{CUBA}}^{\mathrm{H}} \cdot \boldsymbol{\Gamma}_{\mathrm{CUBA}} = M_{\mathrm{Rx}} \cdot \mathbf{I}^{[N_{\mathrm{a2}} \times N_{\mathrm{a2}}]} \qquad (3.5),$$

the Fisher Information Matrix for this special scenario becomes

$$\mathbf{J} = \frac{2}{\sigma^2} \begin{bmatrix} \dfrac{|\gamma|^2 \cdot M_{\mathrm{Rx}} \cdot (N_2^2 - 1)}{12} & 0 & 0 \\ 0 & M_{\mathrm{Rx}} & 0 \\ 0 & 0 & M_{\mathrm{Rx}} \end{bmatrix} \qquad (3.6).$$

In this simple case there are no cross correlations between the parameters and the CRLBs of the parameters are:

$$\mathrm{CRLB}_{\varphi_1} = \frac{\sigma^2}{|\gamma|^2} \frac{6}{M_{\mathrm{Rx}} \cdot (N_2^2 - 1)} \qquad (3.7)$$

$$\mathrm{CRLB}_{\operatorname{Re}\{\gamma_1\}} = \frac{\sigma^2}{2 M_{\mathrm{Rx}}} \qquad (3.8)$$

$$\mathrm{CRLB}_{\operatorname{Im}\{\gamma_1\}} = \frac{\sigma^2}{2 M_{\mathrm{Rx}}} \qquad (3.9).$$

With this example the single path resolution can be evaluated. For multiple path scenarios and real antenna arrays such a simple analytic expression can not be found. Therefore, the described method based on measured characteristics has to be used to calculate the CRLB of the channel model parameters.

4 Conclusions

The described method based on CRLB allows to evaluate arbitrary antenna arrays in single and multiple path scenarios. This approach can also be used to calculate the variance of parameter estimates throughout high-resolution channel parameter estimation. This is of specific interest in coherent multi path scenarios, where the paths are close in terms of the maximum possible resolution since the resulting variance may be rather big (and thus indicate unreliable results) depending on the phase difference between the collocated paths.

The second part of this paper [16] introduces some special measurement scenarios to demonstrate the application of this method for performance evaluation of a real ULA. This measurements have been carried out using the MEDAV RUSK sounder [15].

5 References

[1] Steinbauer M., Molisch A. F., Bonek E., "The Double-Directional Radio Channel", IEEE Antennas and Propagation Magazine, vol. 45, pp. 51-63, No.4, Aug. 2001

[2] Thoma R.S., Hampicke D., Richter A., Sommerkorn, Trautwein U., "MIMO Vector Channel Sounder Measurement for Smart Antenna System Evaluation", European Transactions on Telecommunications ETT, Vol. 12, No. 5, Special Issue on Smart Antennas, pp. 427-438, Sept./Oct. 2001

[3] Thoma R.S., Hampicke D., Landmann M., Richter A., Sommerkorn G., "Measurement-based Channel Modelling (MBPCM)", ICEAA 2003, Torino, Sept. 2003

[4] Richter A., Thoma R., "Parametric Modeling and Estimation of Distributed Diffuse Scattering Components of Radio Channels", COST 273 Temporary Document TD(03)198 , Prague, Czech Republic

[5] Haardt M., Thoma R.S., Richter A., "Multidimensional High-Resolution Parameter Estimation with Applications to Channel Sounding. In High-Resolution and Robust Signal Processing", Marcel Dekker, 2003

[6] Fleury B.H., Dahlhaus D., Heddergott R., and Tschudin M., "Wideband angle of arrival estimation using the SAGE algorithm," in Proc. IEEE Fourth Int. Symp. spread Spectrum techniques and Applications (ISSSTA'96), Mainz, Germany, pp. 79-85, Sept. 1996.

[7] Pedersen K., Fleury B., Mogensen, P. "High resolution of electromagnetic waves in time-varying radio channels". In: Proceedings from the 8th IEEE International Symposium on Personal, Indoor and Mobile Radio Communications (PIMRC'97), Helsinki, Finland, 1-4 September, 1997. Piscataway, NJ, IEEE, 1997, 650-654.

[8] Landmann M., Richter A., Thoma R.S., "Estimation Of Multidimensional Polarimetric Channel Model Parameters", COST 273 Temporary Document, TD(02) 132, Lisbon, Portugal, September 2002.

[9] Richter, A., Landmann M., Thoma, R.S., "A Gradient Based Method for Maximum Likelihood Channel Parameter Estimation from Multidimensional Channel Sounding Measurement," XXVIIth URSI General Assembly, Maastricht, NL, pp. CD, August 2002.

[10] Richter A., Hampicke, D., Sommerkorn G., Thoma R., "Joint Estimation of DoD, Time-Delay, and DoA for High-Resolution Channel Sounding," IEEE VTC2000-Spring, Tokyo, Japan, Vol. 2, pp. 1045-1049, May 2000.

[11] Tan C. M., Landmann M., Richter A., Pesik L., Beach M. A., Schneider Ch., Thoma R. S., and Nix A. R., "On the Application of Circular Arrays in Direction Finding Part II: Experimental evaluation on SAGE with different circular arrays" 1st Annual COST 273 Workshop, Espoo, Finland, May 2002

[12] Scharf Lois L., " Statistical Signal Processing: detection, estimation, and time series analysis ", Addison-Wesley, New York, 1991, ISBN 0-201-19038-9

[13] Stoica P., Nehorai T., "Performance Study of Conditional and Unconditional Direction-of-Arrival Estimation", IEEE Trans. On ASSP, Vol. 38, No. 10, October 1990

[14] Richter A., Thoma R., "Angle Estimation With Circular Uniform Beam Arrays Using the CUBA ESPRIT," Millenium Conference on Antennas & Propagation AP, Davos, Switzerland, pp. CD, April 2000.

[15] http://www.channelsounder.de

[16] Sommerkorn G., Landmann M., Richter A., Thoma R., "Performance Evaluation of Real Antenna Arrays for High-Resolution DoA Estimation in Channel Sounding - Part 2: Experimental ULA Measurement Results", COST 273 Temporary Document, TD(03)196 , Prague, Czech Republic